



ISSN: 0067-2904

## Sedimentological, Mineralogical, and Geochemical characters of the Tigris River floodplain sediment in the Al-Alam area-Tikrit, Northern Iraq

Taher Mahmood Taha\*<sup>1</sup>, Mohanad Rasim Al-Owaidi<sup>2</sup>, Faaq Hassan mahmeed<sup>3</sup>

<sup>1</sup>Department of Applied Geology, College of Science, University of Tikrit, Tikrit, Iraq

<sup>2</sup>Department of Applied Geology, College of Science, University of Babylon, Hilla, Iraq

<sup>3</sup>Department of Applied Geography, College of Art, University of Tikrit, Tikrit, Iraq

Received: 16/6/2022

Accepted: 15/10/2022

Published: 30/8/2023

### Abstract

The mineralogical investigation, geochemical analysis, and grain size calculation were carried out for floodplain sediment in the Tigris River to identify the properties of the sediment. The average values of the three main sediment classes, very fine sand, silt, and clay are 9.67, 62.53 and 27.80%, respectively. The silt size fraction was predominant. The classification and nomenclature of surface sediment types from the floodplain of the Tigris River are sandy-silt and mud, and they are the dominant sediment. Statistical parameters of grain size analysis refer to the average of the median values  $3.74 \Phi$  very fine sand; mean in average  $6.16 \Phi$  coarse silt; standard deviation evident by average  $1.30 \Phi$  poorly sorted, skewed; in average  $-0.14$  negatively skewed, and the average of Kurtosis 2.80 very leptokurtic. The samples analysed by the XRD technique revealed clay minerals (chlorite, illite, montmorillonite, and kaolinite) and non-clay minerals (quartz, feldspar, calcite, and dolomite). The heavy minerals identified as species were zircon, tourmaline, rutile, garnet, olivine, hornblende, pyroxene, kyanite, and magnetic particles. The concentration of major oxides by geochemical analysis indicates a high content of  $\text{SiO}_2$  and  $\text{CaO}$  in the floodplain of the Tigris river.

**Keywords:** Partials size distribution, Mineralogy, geochemistry, Tigris, Al-Alam

## الخصائص الرسوبية والمعدنية والجيوكيميائية لرواسب السهول الفيضية لنهر دجلة في منطقة العلم-تكريت، شمال العراق

ظاهر محمود طه\*<sup>1</sup>، مهند راسم العوادى<sup>2</sup>، فائق حسن محمد<sup>3</sup>

<sup>1</sup>قسم علم الارض، كلية العلوم، جامعة تكريت، تكريت، العراق

<sup>2</sup>قسم علم الارض، كلية العلوم، جامعة بابل، بابل، العراق

<sup>3</sup>قسم علم الارض، كلية العلوم، جامعة تكريت، تكريت، العراق

### الخلاصة

تم اجراء دراسة معدنية ووتحليل جيوكيميائي وحجمي لرواسب السهول الفيضية في نهر دجلة للتعرف على خصائص الرسوبيات. كانت معدل القيم لفئات الرواسب الثلاثة هي الرمل (الرمل الناعم جدًا) والسلت والطين 9.67، 62.53 و 27.80 % على التوالي. كان جزء حجم السلت هو السائد. تصنيف وتسمية أنواع الرواسب

\*Email: [taher.mahmood@tu.edu.iq](mailto:taher.mahmood@tu.edu.iq)

السطحية من السهول الفيضية لنهر دجلة هي السلت- الرملي والطين ، وهما الرواسب السائدة. تشير المعلمات الإحصائية لتحليل حجم الحبيبات إلى معدل القيم المتوسطة  $\Phi$  3.74 رمال ناعمة جدًا ؛ متوسط  $\Phi$  6.16 سلط خشن؛ والانحراف المعياري بمتوسط  $\Phi$  1.30 فرز بشكل سيئ ، والانحراف؛ في المتوسط -0.14 منحرف سلبيًا ، ومتوسط التفرطح 2.80 شديد التفرطح. أظهرت العينات التي تم تحليلها بواسطة تقنية الأشعة السلية الحادثة ان المعادن الطينية (كلوريت ، إيليت ، مونتوريلونيت ، كاولينيت) ومعادن غير طينية (كوارتز ، الفلسبار ، الكالسيت والدولوميت). المعادن الثقيلة التي تم تحديدها هي الزركون ، التورمالين ، الروتيل ، الكارنيت، الاوليفين ، الهورنبلند ، البيروكسين ، الكيانيت ، والمعادن المعتمه. يشير تركيز الأكاسيد الرئيسية عن طريق التحليل الجيوكيميائي إلى وجود محتوى عالٍ من السليكا والجير في السهول الفيضية لنهر دجلة.

## 1. Introduction

Many researchers, among them, have studied the sediment of the Tigris River Berry et al. [1], Philip [2], Banat [3], Ali [4], Hana and Al-Hilali [5], and Yousif [6]. In the terrestrial environment, the fluvial systems represent the dominant transportation media. The understanding the properties of modern fluvial deposits, it is critical to understand their roles in various environmental activities, especially sediment transport and related pollutants [7]. Sediments also provide information regarding the regional environmental changes in countries that have undergone essential changes in land use and industrial development [8]. Fine-grained sediment (grain size less than 2  $\mu\text{m}$ ) builds floodplains and deltas [9].

The general trend of point-bar deposits is fining-upward, and it is documented to a wide extent, from both modern and ancient rivers, preserved successions. In other sedimentary systems, however, the general pattern may not occur in mud-dominated systems and instead emerge as alternate coarsening-upward trends [10]. The grain-size properties of surface sediment refer to the sediment transportation, deposition and redistribution processes and include much information about sediment provenance, the change in sea level, the dynamic environment and transport pathways [11].

The recent sediment may have derived from older rock (igneous, metamorphic or sedimentary), which outcropped on the earth's surface by weathering and erosion [12]. The composition of sediment is primarily controlled by the source rock composition, in addition to the weathering, transport and diagenetic processes to a minor extent [13]. The goal is to study the character of this sediment in terms of texture and classification, investigate the mineralogy by identifying clay minerals and non-clay minerals, determine the heavy mineral type, and determine a provenance-based mineral investigation and geochemistry by studying the major oxide in the fine grain part of the sediment.

## 2. Geological Setting

From the tectonic point of view, the studied area is located in the Unfolded Zone, according to [14]. The Tigris River is parallel to subsurface anticlines like Ajal and Tikrit, which affects the study area's southern part [15]. The two main outcrops in the area are the Euphrates and Jeribe formations (Lower Miocene), exposed at the core of the Makhul Anticline with a 55m thickness and mainly composed of limestone and evaporite. In addition, the Fatha Formation (Middle Miocene) is exposed on both sides of the Tigris River from Hammam Al-Alial to the Fatha Carriage, which was formed by the alternative of evaporite facies alternating with limestone, marl and fine clastic [16].

Many cycles of evaporite, limestone, and marl deposits and a marly-lagoonal represent them. The Injana Formation (Upper Miocene) is outcropped in many sites and is formed of alternatives of sandstone, siltstone, and claystone [17] and contains thin lenses of secondary

gypsum. It is deposited in a fluvial continental environment with a thick clastic sedimentary succession. The Mukdadiya Formation (Pliocene) is exposed on the eastern side of the Tigris River and on both sides of the Hemrin Anticline. It is formed of pebbly sandstone, gravel, siltstone and claystone, which is deposited in the continental environment [15].

Quaternary deposits (Pleistocene) form terraces on both sides of the Tigris River, and the floodplain extends for a wide distance to the east and west of the river. Quaternary deposits consist of clastic rich in gypsiferous materials [15]. It is formed of a mixture of gravel, sand and clay as horizontal lenses with terraces of different elevations on both sides of the river. The maximum elevation of the old terraces is about 35m above the water level of the river at present.

### 3. Materials and Methods

The Tigris floodplain sediments are unconsolidated. Floodplain sediments were sampled from a section (along with the downstream) on a natural outcrop of the Tigris riverbank. Sampling has been done along the river's east bank, consisting of the front of the floodplain, to represent the spatial variation of the floodplain sediment. Twelve samples were collected in October 2019 at a minimum flow (Figure 1).

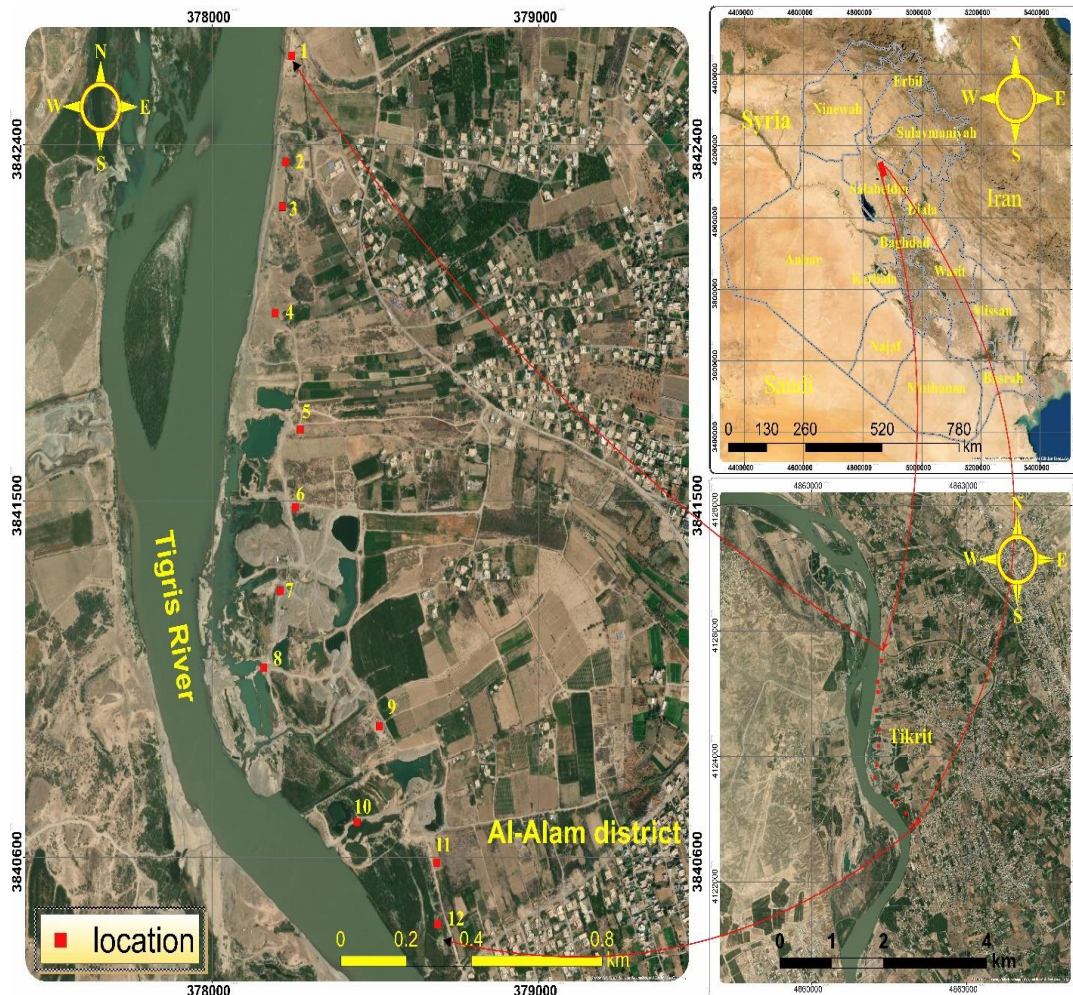


**Figure 1:** Location and number identification samples of the study area

All samples are represented by flood events that deposit new top-layer materials deposited in the last river flooding in April (Figure 2). The samples were carefully selected to avoid pollution resulting from human activity, as represented in agricultural fields, quarries, and levees. In

addition, take about 2 kg of weight and keep it in a plastic bag. The samples were left to dry at room temperature in the original plastic bag.



**Figure 2:** Collected samples in the study area (locations site 1, 2, 5)

Some aggregate was formed during drying; a porcelain mortar and pestle were used to disaggregate it. In total, 12 samples were selected for textural analysis, six samples for geochemical analysis, and eight samples for heavy mineral identification. The sampling stations were geo-referenced using the global positioning system (GPS) Table 1.

The samples were dried at room temperature after being divided into two parts and taking one part for sieve analysis. 150 gm from each sample were subjected to wet sieve analysis to separate the very fine particles of silt and clay (0.0630–0.0004 mm), and the grains passing through the sieve (more than 0.0620 mm) were pipette analyzed according to Stock's law.

**Table 1:** Coordinate of collected samples

Sample No.	Location	
	Latitude (N)	Longitude E
1	34.718108	43.670338
2	34.71559	43.670241
3	34.714513	43.670043
4	34.712163	43.669953
5	34.709905	43.670547
6	34.708025	43.670379
7	34.705825	43.670049
8	34.704275	43.669681
9	34.703206	43.67351
10	34.700929	43.672429
11	34.700091	43.675148
12	34.698416	43.675586

Distilled water and 10 ml of 0.05 M Na-hexametaphosphates ( $\text{NaPO}_3$ )<sub>6</sub> were used before analysis to avoid particles' flocculation. Calculate the weight percentage for each size particle class using the Phi-scale to classify these sediments. Cumulative frequency plots were made on a semi-probability scale, and Phi ( $\Phi$ ) values at 5, 16, 25, 50, 75, 84, and 95th were obtained from this plot, and calculated statistical parameters using the method of Folk and Ward [18]. Grain size analysis was carried out at the University of Tikrit, Applied Geology Department, sedimentology and optical mineralogy labs.

X-Ray Diffractometers (XRD) and heavy mineral analysis were used to investigate the mineralogy. The XRD analysis was performed at the XRD Lab of the Ministry of Sciences and Technology. Six samples with a higher clay percentage were chosen and analyzed for clay mineral analysis using XRD with three different treatments. Heavy mineral separation was carried out on samples containing more than 10 g of very fine sand (0.125–0.063 or 3.0–4.0 mm) by traditional gravity methods using Bromoform liquid (CHBr<sub>3</sub>, Specific Gravity 2.89). The magnetic particles from the heavy part are separated by using a magnet. The thin section of the heavy mineral is made using Canada balsam identification of the heavy mineral using a polarizing microscope. Every specimen counts more than 200 grains. This procedure is carried out at the University of Tikrit, Department of Applied Geology, Optical Mineralogy Lab. The samples that contain a greater abundance of fine fractions (silt and clay) were selected for chemical analysis (major oxides) at the University of Baghdad, Geology Department, Geochemical Lab. The determination of the percentages of the major oxides SiO<sub>2</sub>, Al<sub>2</sub>O<sub>3</sub>, Fe<sub>2</sub>O<sub>3</sub>, TiO<sub>2</sub>, MgO, CaO, K<sub>2</sub>O, MnO, Na<sub>2</sub>O, and P<sub>2</sub>O<sub>5</sub> were done by X-ray fluorescence (XRF) spectrometer. Twelve soil samples were selected and pulverized into a fine powder for testing by the XRF instrument. The samples were pressed to a special disc for an XRF examination by a SPECTRO XPOS tool (Germany-made). Then, these oxides are normalized to the upper continental crust (UCC) composition [19].

## 4. Results and Discussions

### 4.1. Sedimentological study

Table 2 and Figure 3 (A and B) display the distribution of individual particle size classes in the studied samples. The Tigris flood plain sediments consist mostly of mud (silt and clay particles) with little sand.

**Table 2:** wt. % for particle size categories of studied samples and calculated statistical parameters

Sample No.	Particles size categories				Statistical Parameter			
	Sand	Silt	Clay	Median	Mean	Standard Deviation	Skewness	Kurtosis
	%			$\Phi$				
1	11.82	45.33	42.85	3.03	5.70	1.45	-0.17	3.54
2	18.57	46.40	35.04	2.64	5.56	1.64	-0.26	4.56
3	27.53	64.60	7.88	2.67	5.73	1.84	-0.44	6.79
4	2.34	62.67	34.99	4.41	6.25	1.11	-0.08	2.01
5	8.39	90.67	0.94	3.66	7.04	1.18	-0.22	1.96
6	9.39	42.98	47.63	3.47	5.69	1.31	-0.07	2.88
7	10.33	84.07	5.60	3.38	6.82	1.24	-0.20	2.23
8	7.83	59.48	32.70	3.61	6.06	1.36	-0.21	2.92
9	0.00	42.20	57.80	5.19	6.10	0.78	0.40	0.92
10	19.02	76.09	4.89	2.93	6.01	1.80	-0.47	2.60
11	0.61	74.37	25.02	4.93	6.59	0.99	-0.05	1.59
12	0.26	61.47	38.27	4.93	6.34	0.97	0.09	1.57
Min.	0.00	42.20	0.94	2.64	5.56	0.78	-0.47	0.92
Max.	27.53	90.67	57.80	5.19	7.04	1.84	0.40	6.79
Average	9.67	62.53	27.80	3.74	6.16	1.30	-0.14	2.80

The average values of the three main classes were sand (very fine sand), silt, and clay, which were 9.67%, 62.53%, and 27.80%, respectively. As a result, silt-sized particles dominate on average. The proportions of sand, silt and clay fractions in the flood plain sediments indicate

an unsorted nature [13]. The Folk's [20] classification and nomenclature of surface sediment types in the study area are shown in Figure 3A. The figure illustrates the mud fraction (clay and silt) increase against the sand fraction. Also, four primary sediment types were identified in the study area, sandy silt, sandy mud, silt, and mud. Sandy silt and mud are the dominant sediment types. Mud is mainly distributed in areas with more silt content than clay. Grain size distribution is a critical physical property of sediment that plays a key role in understanding sediment erosion, transport, accumulation, and riverbed evolution [21].

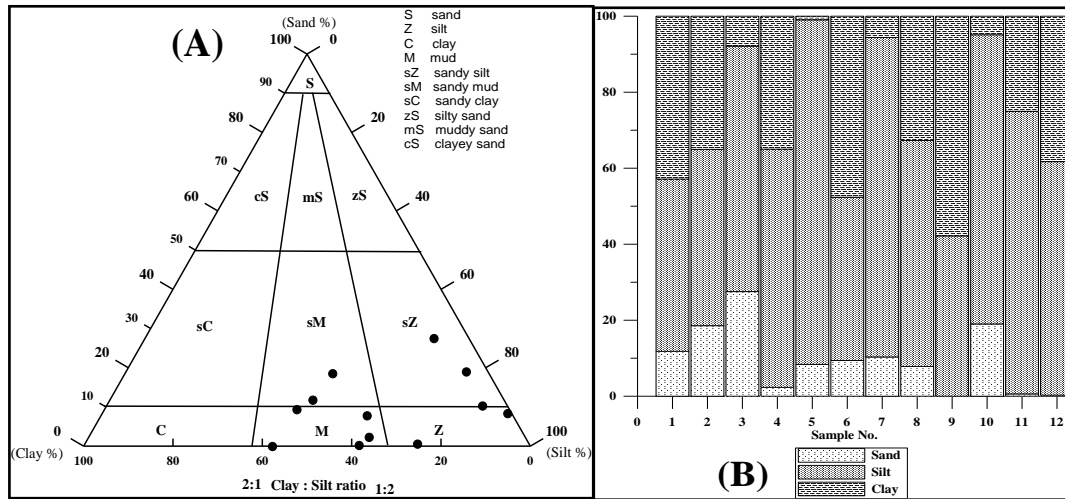


**Figure3:** (A) Nomenclature (After [18]) and (B) Bar chart showing Textural properties of studied samples.

The sediment that represents a bed load consists of the grain that is transported in rolling, sliding, and saltation ways on or near the river bed during the active channel. The suspended load is transported by turbulent flow and local flow velocities. The collected sediment samples from the subsurface of a river's active channel were classified as bed load sediments. The samples gathered to form the top of sand bars or from an overbank are classified as suspended load sediment [22]. Therefore, all the studied samples were classified as suspended loads. That corresponds with the predominating mud size against course size in studied samples.

Grain size is a sediment characteristic determined more by the nature of the source area than by the transportation process or the depositional environment [23]. The Tigris River and its tributaries flow through a crystalline rock-covered area. The composition of overbank sediment from the Tigris River floodplain may result from the high-energy flow, which brings and entraps various size grains of sediment from the catchment area in the stream, mixing thoroughly, and the sudden decrease in river flow, which dumps on the bank [24]. The nature of the source, the degree of weathering (physical and chemical), the hydrodynamic condition during sediment deposit, and the manner of formation (architecture) of the flood plain are all factors that influence the textural properties of Tigris river floodplain sediments [24], [25]. The statistical parameters of grain size analysis are shown in Table 2. Median values of sediment range between 2.64  $\Phi$  and 5.19  $\Phi$ , which refers to fine sand to coarse silt, with an average of 3.74  $\Phi$  for very fine sand. The mean value ranged between 5.56  $\Phi$  and 7.04  $\Phi$  indicted coarse silt to medium silt, with an average of 6.16  $\Phi$  coarse silt. The lower clay content in some samples suggests that these small particles were removed during the flooding period [26]. The sorting of flood plain sediment provided by standard deviation ranges from 0.78  $\Phi$  moderately sorted to 1.84  $\Phi$  poorly sorted, on average of 1.30  $\Phi$  poorly sorted. A wide range of skewness values was obtained from studied samples of the flood plain sediment, ranging between -0.47, very negatively skewed, and 0.40, very positively skewed, on average -0.14,

negatively skewed. Skewness can be used to distinguish between the symmetry of a distribution symmetry and to determine the cause of sedimentation [27]. Fine sediment predominates slightly more than coarse sediment, indicating a positive bias. Kurtosis values vary from 0.92 to 6.79, indicating mesokurtic to extremely leptokurtic, with an average of 2.80 leptokurtic. The very fine size of sediment is due not only to the results of the degree of transport but also to the predominant chemical weathering in the source area, which does not yield coarse sediment [26].

#### *4.2. Mineral composition Tigris of floodplain sediment*

Weathering parent rocks exposed in the river and tributary catchment areas produce sediment grains. Quartz, calcite, dolomite, and feldspar are the main components of coarse grains derived from physical weathering and found within a silicate skeleton based on the mineral composition of the parent rock. In contrast, the fine particles were the product of chemical weathering and represented different clay mineral types (montmorillonite, chlorite, kaolinite, and illite). The dissimilarity in the crystal structures of coarse and fine grains results in variations in their physical and chemical properties and results in variations in their modes of transport and sedimentation processes.

##### *4.2.1 XRD analysis*

The XRD results show clay minerals in the studied samples, including chlorite, illite, montmorillonite, and kaolinite. In addition, some other non-clay minerals appear, including quartz, feldspar, calcite, and dolomite (Figure 4). In this study, chlorite and illite clay minerals were found in six samples, whereas montmorillonite and kaolinite appeared only in samples 4 and 6, respectively. When rocks composed of feldspar and plagioclase, such as anorthite, are subjected to weathering, they produce kaolinite [28]. The studied samples are characterized by non-clay minerals (quartz, feldspar, calcite, and dolomite), which are dominant in all the samples. The grain size distribution can easily estimate the mineral composition [29].

The main components of physical weathering results are coarse grains, quartz, calcite, and feldspar. At the same time, chemical weathering produces fine particles that are made of clay minerals (montmorillonite, kaolinite, and illite) [29]. They are omnipresent in soils, fine-grained argillaceous sediments, and shales and are formed through weathering and hydrothermal alteration of felsic and mafic rocks, respectively, or by direct sedimentation in a marine environment [30].

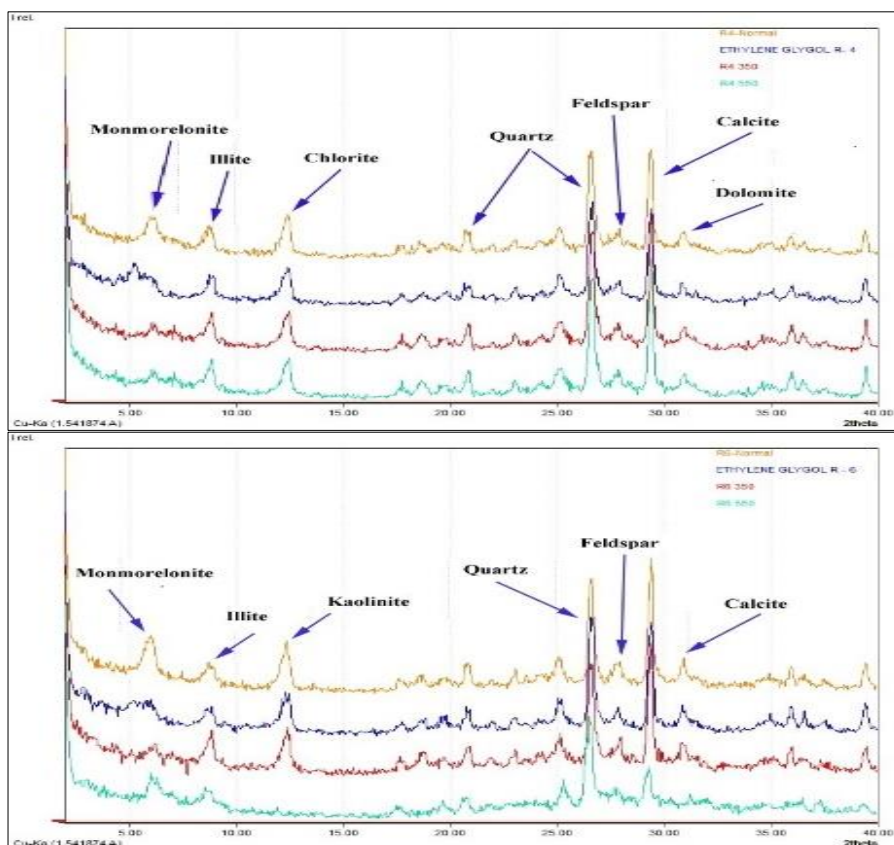


**Figure 4 :** XRD plot of the sediments from the floodplain, Tigris River (S-4&6)

Clay mineral composition gives valuable information regarding the types of weathering and intensity, which are directly identified by various climatic conditions (rainfall, temperature), rock composition, and tectonic activity [31]. The product of weathering some non-clay minerals, maybe form clay minerals. For instance, under various soil environments, feldspar can form clay minerals such as sericite, illite, and kaolinite [29]. The products of the weathering of crystalline rocks (igneous and metamorphic rocks) are mostly illite and chlorite minerals [21]. Kaolinite is mostly thought to occur in tropical climates from well-developed ferrallitic soils in a plain environment with intense hydrolysis processes [32]. The alteration of volcanic rock-derived smectite can be a good indicator of volcanic sediment sources [21]. The abundance of secondary weathered products such as phyllosilicates and clay indicates the high degree of weathering of sediment. Both illite and chlorite are present at a higher rate of physical weathering and relatively moderate chemical weathering processes [33]. Physical bedrock erosion is strongly linked to a dry, cold environment [21]. The non-clay minerals have been derived from the rock bed exposed in the river channel in the upstream direction. Calcite and dolomite have another source of authigenically formation in sediment, such as precipitation as cement material after being deposited. In contrast, quartz and feldspar come from the weathering parent crystalline rock exposed in the river basin and the bedrock in the channel.

#### 4.2.2 Heavy Minerals

The heavy mineral percentages on average and the type of species assemblage in the studied samples were composed of zircon (2.67%), tourmaline (27.94%), rutile (1.22%), garnet (25.82%), olivine (20.15%), hornblende (16.56%), pyroxene (2.12%), and kyanite (3.52%) as shown in Figure 5. In addition to the magnetic partials, understanding heavy mineral preservation is important for interpreting the origin, pathways, provenance, and geochemistry [34].

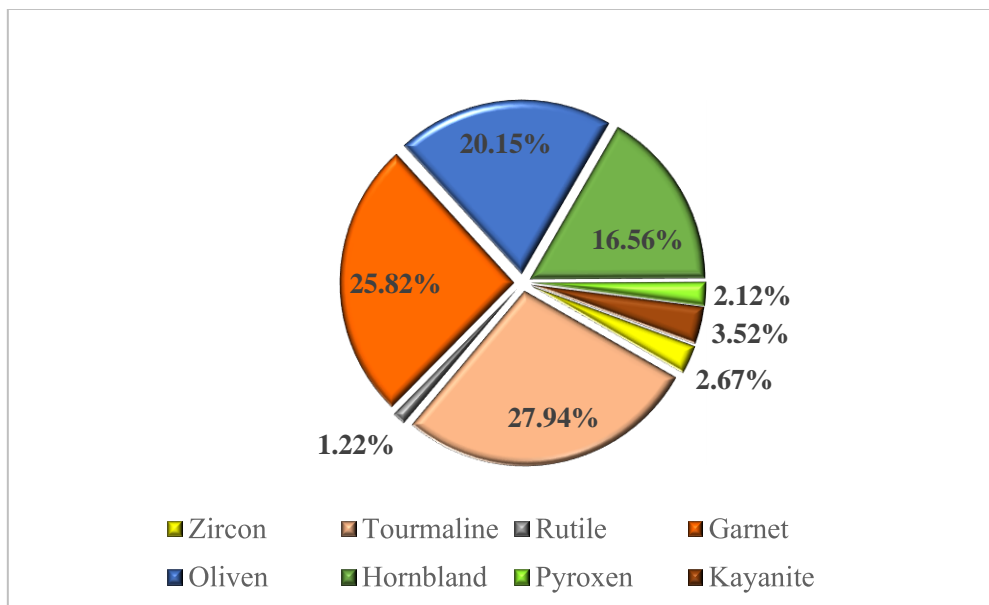


**Figure 5:** Average percentage of heavy mineral species in the studied samples

In detrital sediment, the distribution of heavy minerals is controlled by factors such as the type of base rock, the crystal mineral size, sorting by the hydraulic, the density of minerals, and mineral fragmentation [35]. In the studied samples, the most abundant are tourmaline, garnet, olivine, and hornblende, while the others are rare. Because of the wide distribution of garnet in different grain sizes, they reflect parent rocks, which belong to the Mesozoic clastic deposits [35]. The three predominant heavy minerals (tourmaline, garnet, and olivine) reflected the varied source types of the sediment. Zircon, tourmaline, and rutile originate in source areas consisting of igneous and/or reworked sedimentary rocks [32]. Pyroxenes are expected to be from an ultramafic source but are probably lacking due to their low stability during burial diagenesis [36]. Higher concentrations of heavy minerals are in channel fill rather than over bank deposits. Andò [37] found that fast-settling ultra-stable minerals like zircon are preferentially concentrated in channel-fill deposits, whereas the tops of overbank deposits are notably enriched with slow-settling platy phyllosilicate (mineral and geochemical data). This interpretation is supported by the low percentage of zircon and rutile in the studied samples.

#### 4.3 Major Oxides

The flood plain's sediments from the Tigris River, the major element components of the mud fraction, are provided in Table 3.

**Table 3:** Major oxides content (wt. %) in floodplain sediments for selected studied samples

Major Oxide		Sample number						Statistical Parameter		
		1	2	4	6	9	12	Min.	Max.	Average
SiO <sub>2</sub>	%	43.01	42.57	48.75	46.24	46.68	45.77	42.57	48.75	45.50
Fe <sub>2</sub> O <sub>3</sub>		4.39	4.28	7.59	5.80	3.81	4.63	3.81	7.59	5.08
Al <sub>2</sub> O <sub>3</sub>		12.98	13.60	17.18	15.14	14.11	15.56	12.98	17.18	14.76
TiO <sub>2</sub>		0.61	0.15	0.66	0.16	0.58	0.54	0.15	0.66	0.45
K <sub>2</sub> O		2.17	1.19	2.88	1.50	1.75	2.01	1.19	2.88	1.92
CaO		27.33	26.89	11.17	23.66	25.48	23.65	11.17	27.33	23.03
Na <sub>2</sub> O		3.58	3.78	3.01	3.02	2.06	2.95	2.06	3.78	3.07
MgO		2.67	3.58	6.26	2.32	2.53	2.24	2.24	6.26	3.26
MnO		0.11	0.10	0.10	0.10	0.10	0.10	0.10	0.11	0.10
P <sub>2</sub> O <sub>5</sub>		0.12	0.16	0.14	0.13	0.11	0.10	0.10	0.16	0.13
SO <sub>3</sub>		0.83	0.83	0.84	0.72	0.95	1.03	0.72	1.03	0.87
Total		97.79	97.13	98.57	98.79	98.16	98.58			

The concentration of major oxides in the studied samples was normalized with Upper Continental Crust (UCC) data that was reported by Taylor and McLennan [19]. The overbank sediment of the Tigris floodplain under investigation reveals a varied geochemical composition, which reflects the control of various sediment logical processes. The SiO<sub>2</sub> in the floodplain sediments varied from 42.57 to 48.75 wt.%, with an average of 45.50 wt.%. It is lower than the UCC value (66.00 wt. %). Fine-grained sediments (mud to silt) have low SiO<sub>2</sub> content, while larger grain sizes have higher SiO<sub>2</sub> content [38].

The TiO<sub>2</sub> was relatively lower than the UCC, which was also recorded. Al<sub>2</sub>O<sub>3</sub> (8.11 to 12.18 wt.%) and average 10.09 wt. %, and K<sub>2</sub>O (1.19 to 2.88 wt. %) and average 1.92 wt. %, both oxides have lower content than UCC, indicating that the samples have fewer clay minerals. The CaO has a very high content of 11.17 to 27.33% wt%, with an average of 23.00 wt% more than the UCC average (3.59 wt%). It can be attributed to the detrital carbonate derived from carbonate rock exposed in the Tigris channel or catchment area or pedogenic carbonate from the soils, in addition to the CaO in the other phases of rock-forming minerals in the silicate fraction. Na<sub>2</sub>O ranged from 2.06 to 3.78 wt. % with an average of 3.07 wt. %, which corresponds with the UCC average (3.27 wt. %), Na<sub>2</sub>O more than K<sub>2</sub>O reflects the low content of K-bearing phases such as K-feldspar and clay mineral-bearing potassium in the mud fraction from the floodplain sediment of the Tigris River. MgO oxide content ranges from 2.24 to 6.26 wt %, with an average of 3.26 wt %, representing values higher than the UCC. It attributed to the dolomite presence in the mud fraction. Fe<sub>2</sub>O<sub>3</sub> is relatively more abundant than UCC, with content fluctuating from 4.59 to 3.42 wt. % and an average of 5.04 wt. %.

The relatively higher content results from the abundance of Fe-bearing minerals, such as iron oxides (hematite, goethite) or siderite (FeCO<sub>3</sub>) in the detrital carbonate grain. The variation of MnO and P<sub>2</sub>O<sub>5</sub> was not significant in all samples, as shown by the UCC-normalized major element patterns (Figure 6). The average abundances of TiO<sub>2</sub>, Fe<sub>2</sub>O<sub>3</sub>, MnO, MgO, CaO, and P<sub>2</sub>O<sub>5</sub> tended to decrease with increasing grain size [38]. It is very important to understand the behavior of elements in various mineral phases during the sedimentary processes, weathering of source rock, transportation, and deposition of derived sediment [24].

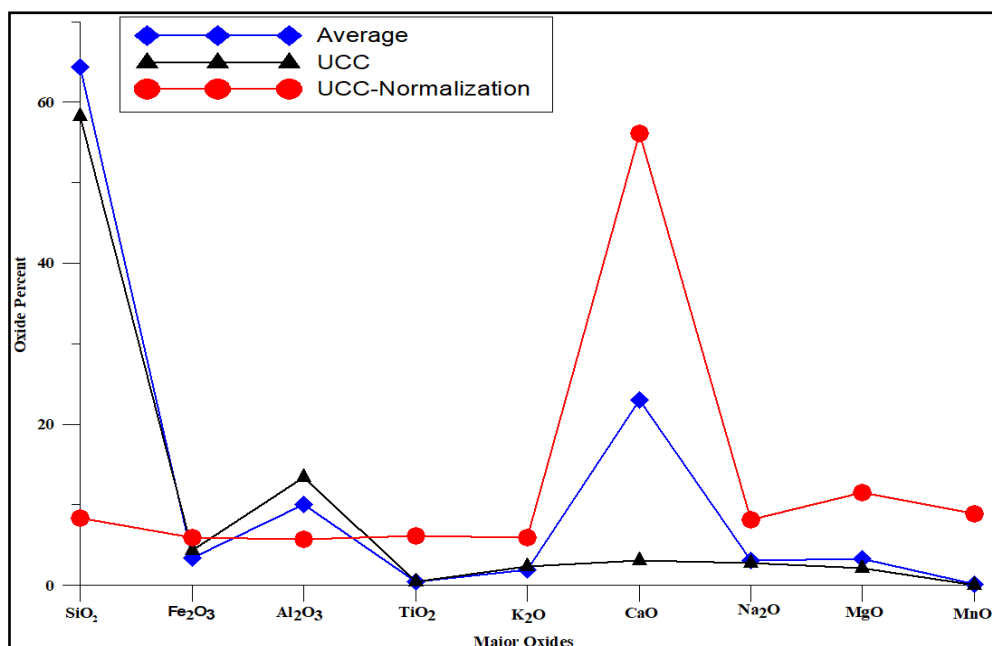


**Figure 6:** UCC normalization with average major oxides of the sediments of Tigris flood plain.

SiO<sub>2</sub> versus Na<sub>2</sub>O and K<sub>2</sub>O (correlation coefficients  $r = -0.02$  and  $r = -0.23$ , respectively,  $n = 12$ ) is not statistically significant (Table 4), referring to the high mobility of Na and K during weathering. The negative relationship between SiO<sub>2</sub> and Al<sub>2</sub>O<sub>3</sub> ( $r = -0.45$ ,  $n = 12$ ) indicates that the detrital quartz grains is represented most of the silica [26]; [27]. The negative relationship between SiO<sub>2</sub> and TiO<sub>2</sub>, Fe<sub>2</sub>O<sub>3</sub>, and MnO in the floodplain sediment may indicate that most SiO<sub>2</sub> is related to quartz grains rather than the clay component [38].

**Table 4:** Statical correlation of major oxides of the Tigris River sediments

	SiO <sub>2</sub>	Fe <sub>2</sub> O <sub>3</sub>	Al <sub>2</sub> O <sub>3</sub>	TiO <sub>2</sub>	K <sub>2</sub> O	CaO	Na <sub>2</sub> O	MgO	MnO	P <sub>2</sub> O <sub>5</sub>	SO <sub>3</sub>
SiO <sub>2</sub>	1.00										
Fe <sub>2</sub> O <sub>3</sub>	-0.62	1.00									
Al <sub>2</sub> O <sub>3</sub>	-0.45	0.89	1.00								
TiO <sub>2</sub>	-0.03	0.44	0.39	1.00							
K <sub>2</sub> O	-0.23	0.81	0.75	0.83	1.00						
CaO	0.07	-0.81	-0.73	-0.40	-0.78	1.00					
Na <sub>2</sub> O	-0.02	-0.13	0.12	-0.39	-0.15	0.17	1.00				
MgO	0.26	0.49	0.47	0.29	0.64	-0.86	0.14	1.00			
MnO	-0.37	-0.02	-0.03	0.34	0.21	0.35	0.42	-0.19	1.00		
P <sub>2</sub> O <sub>5</sub>	0.36	-0.19	-0.16	-0.55	-0.22	-0.17	0.61	0.54	-0.15	1.00	
SO <sub>3</sub>	0.42	-0.15	0.07	0.53	0.16	0.07	-0.43	-0.18	-0.19	-0.63	1.00

## 5. Conclusions

The main sediment of the Tigris floodplain consists entirely of mud (silt and clay-sized particles) with little sand. However, on average, silt-sized particles are predominant. The classifications of the four primary sediment types were: sandy silt, sandy mud, silt, and mud. Sandy silt and mud are the dominant sediment types. Mud is mainly a type with a higher silt content than clay. Statistical parameters by an average of grain size analysis refer to the median of 3.74  $\Phi$  very fine sand; mean of 6.16  $\Phi$  coarse silt; the standard deviation of 1.30  $\Phi$  poorly sorted; skewed -0.14 negatively skewed; and kurtosis of 2.80 very leptokurtic.

The mineralogical study, by XRD analysis, revealed that clay minerals, including chlorite, illite, montmorillonite, and kaolinite, were abundant. Non-clay minerals, including quartz, feldspar, calcite, and dolomite. The components of eight clay mineral samples are identified by chlorite and illite in all samples, whereas montmorillonite and kaolinite appear only in samples 4 and 6, respectively. The heavy mineral percentages were zircon (2.67%), tourmaline (27.94%), rutile (1.22%), garnet (25.82%), olivine (20.15%), hornblende (16.56%), pyroxene (2.12%), and kyanite (3.52%). Tourmaline, garnet, olivine, and hornblende are more common than the others.

The major oxide of sediment with a normalization pattern shows SiO<sub>2</sub> (42.57 to 48.75 wt. %) with an average of 45.50 wt. % lower than the UCC value (66 wt. %) and CaO (11.17 to 27.33 wt. %), with an average of 23.00 wt. % more than the UCC average (3.59 wt. %) in the floodplain of the Tigris river. All samples were insignificant in the average variance of TiO<sub>2</sub>, Fe<sub>2</sub>O<sub>3</sub>, MnO, MgO, and P<sub>2</sub>O<sub>5</sub>.

## 6. Acknowledgements

We are very grateful to our friends for assisting in fieldwork. We are also grateful to Dr. Lafta Salman for his discussion in this research. We would also like to extend our most profound respect and appreciation to all the scientists who have contributed substantially to earlier research papers on the Tigris River's sediment.

## References:

- [1] R. W. Berry, G. P. Brophy and A. Naqash, "Mineralogy of the Suspended Sediment in the Tigris, Euphrates, and Shatt Al-Arab Rivers of Iraq, and the Recent History of the Mesopotamian Plain," *Journal of Sedimentary Research*, vol. 40, no. 1, pp. 131-139, 1970.
- [2] G. Philip, "Mineralogy of Recent Sediments of Tigris and Euphrates Rivers and Some of the Older Detrital Deposits," *Journal of Sedimentary Research*, vol. 38, no. 1, pp. 35-44, 1968.
- [3] K. M. Banat, "Geochemical Study of Heavy Metals and Major Ions from the Tigris River between Baghdad and Mosul," *Iraqi Geological Society*, no. Special Issue, pp. 47-56, 1977.
- [4] J. A. Ali, "Comparative Study between Recent Sediment of Euphrates and Tigris River and Ancient Sediment of Old Red Sandstone (Midland Valley of Scotland)," *Iraqi Journal of Science*, vol. 18, no. 2, pp. 123-130, 1984.
- [5] A. A. Hana and M. A. Al-Hilali, "Distribution of Some Chemical Element in the Sediment in the Mesopotamian Plain Iraq," *Journal of the Geological Society of Iraq*, vol. 19, pp. 267-280, 1986.
- [6] I. A. Yousif, "Opaque Minerals in the Recent Sediment of Euphrates and Tigris Basin," *Iraqi Geological Journal*, vol. 24, pp. 141-148, 1991.
- [7] S. Nehyba, K. Hilscherová, K. Jarkovský, L. Dušek, T. Kuchovský, J. Zeman, J. Klánová and I. Holoubek, "Grain Dize, Geochemistry and Organic Pollutants in Modern Fluvial Deposits in Eastern Moravia (Czech Republic)," *Environmental Earth Sciences*, vol. 60, pp. 591-602, 2010.
- [8] T. Grygar, I. Světlík, L. Lisá, L. Koptíková, A. Bajer, D. S. Wray, V. Ettler, M. Mihaljevič, T. Nováková, M. Koubová, J. Novák, Z. Máčka and M. Smetana, "Geochemical Tools for the Stratigraphic Correlation of Floodplain Deposits of the Morava River in Strážnické Pomoraví, Czech Republic from the Last Millennium," *Catena*, vol. 80, no. 2, pp. 106-121, 2010.
- [9] H. Ma, J. A. Nittrouer, B. Wu, M. P. Lamb, Y. Zhang and D. Mohrig, "Universal Relation with Regime Transition for Sediment Transport in Fine-Grained Rivers," *Earth, Atmospheric, and Planetary Sciences*, vol. 117, no. 1, pp. 1-6, 2019.
- [10] J. Li, J. Vandenberghe, N. P. Mountney and S. M. Luthi, "Grain-Size Variability of Point-Bar Deposits from a Fine-Grained Dryland River Terminus, Southern Altiplano, Bolivia," *Sedimentary Geology*, vol. 403, pp. 105663, 2020.
- [11] P. Yuan, H. Wang, W. U. Xiao and B. I. Naishuang, "Grain-Size Distribution of Surface Sediments in the Bohai Sea and the Northern Yellow Sea: Sediment Supply and Hydrodynamics," *Journal of Ocean University of China*, vol. 19, no. 3, pp. 589-600, 2020.

- [12] E. O. Joshua and O. A. Oyebanjo, "Distribution of Heavy Minerals in Sediments of Osun River Basin Southwestern Nigeria," *Research Journal of Earth Sciences*, vol. 1, no. 2, pp. 74-80, 2009.
- [13] M. E. Mondal, H. Wani and B. Mondal, "Geochemical Signature of Provenance, Tectonics and Chemical Weathering in the Quaternary Flood Plain Sediments of the Hindon River, Gangetic Plain, India," *Tectonophysics*, vol. 566–567, pp. 87-94, 2012.
- [14] S. Z. Jassim and T. Boday, "Units of the Unstable Shelf and Zagros Suture," in *Geology of Iraq*, Brno, Dolin, Prague and Moravian Museum, 2006, pp. 73-90.
- [15] N. M. Hamza, F. A. Lawa, S. Y. Yagoub, A. Z. Mousa and S. S. Fouad, "State Establishment of Geological Survey and Mineral Investigation," *GEOSURV*, Baghdad, 1990.
- [16] A. K. Jamil, H. J. Al-Biaty and A. A. Ali, "Hydrogen Sulphide Pollution of Tigris River –Iraq," *Journal of Water Resources*, vol. 3, no. 2, pp. 73-85, 1984.
- [17] A. Buday, *Regional Geology of Iraq Stratigraphy and Paleogeography*, State Organization of Minerals: Baghdad, 1980.
- [18] R. L. Folk and W. C. Ward, "Brazos River Bar: A Study in the Significance of Grain Size Parameters," *Journal of Sedimentary Research*, vol. 27, pp. 3-26, 1957.
- [19] S. R. Taylor and S. M. McLennan, *The Continental Crust: Its Composition and Evolution*, Palo Alto: Blackwell Scientific Pub, 1985.
- [20] R. L. Folk, "The Distinction between Grain Size and Mineral Composition in Sedimentary-Rock Nomenclature," *The Journal of Geology*, vol. 62, no. 4, pp. 344-359, 1954.
- [21] P. Zhang, W. Yao, G. Liu, P. Xiao and W. Sun, "Geomorphology Experimental Study of Sediment Transport Processes and Size Selectivity of Eroded Sediment on Steep Pisha Sand stone Slopes," *Geomorphology*, vol. 363, pp. 07211, 2020.
- [22] M. Singh, I. B. Singh and G. Müller, "Sediment Characteristics and Transportation Dynamics of the Ganga River," *Geomorphology*, vol. 86, no. 1-2, pp. 144–175, 2007.
- [23] P. McLaren and D. Bowles, "An Interpretation of Trends in Grain Size Measures," *Journal of Sedimentary Petrology*, vol. 51, no. 2, pp. 611–624, 1981.
- [24] C. Maharana, D. Srivastava and J. K. Tripathi, "Geochemistry of Sediments of the Peninsular Rivers of the Ganga Basin and Its Implication to Weathering, Sedimentary Processes and Provenance," *Chemical Geology*, vol. 438, pp. 1-20, 2018.
- [25] P. McLaren, "An interpretation of trends in grain size measures," *Journal of Sedimentary Research*, vol. 51, no. 2, pp. 611-624, 1981.
- [26] D. T. Chougong, A. Zacharie, A. Bessa, G. Ngueutchoua, R. Fouateu, S. Carole and J. S. Armstrong-altrin, "Mineralogy and Geochemistry of Lobe´ River Sediments, SW Cameroon Implications for Provenance and Weathering," *Journal of African Earth Sciences*, vol. 183, pp. 104320., 2021.
- [27] C. Wang, M. Chen, H. Qi, W. Intasen and A. Kanchanapant, "Grain-Size Distribution of Surface Sediments in the Chanthaburi Coast, Thailand and Implications for the Sedimentary Dynamic Environment," *Journal of Marine Science and Engineering*, vol. 8, no. 4, pp. 242, 2020.
- [28] S. S. Barik, P. Prusty, R. K. Singh, S. Tripathy, S. H. Farooq and K. Sharma, "Seasonal and Spatial Variations in Elemental Distributions in Surface Sediments of Chilika Lake in Response to Change in Salinity and Grain Size Distribution," *Environmental Earth Sciences*, vol. 79, no. 11, pp. 269, 2020.
- [29] S. Tian, Z. Li, Z. Wang, E. Jiang, W. Wang and M. Sun, "Mineral Composition and Particle Size Distribution of River Sediment and Loess in the Middle and Lower Yellow River," *International Journal of Sediment Research*, vol. 63, no. 3, pp. 392-400, 2020.
- [30] R. Schliemann and S. V. Churakov, "Atomic Scale Mechanism of Clay Minerals Dissolution Revealed by Ab Initio Simulations," *Geochimica et Cosmochimica Acta*, vol. 239, pp. 438-460, 2021.
- [31] E. Garzanti, M. Padoan, M. Setti, A. López-Galindo and I. M. Villa, "Provenance versus Weathering Control on the Composition of Tropical River Mud (Southern Africa)," *Chemical Geology*, vol. 366, pp. 61-74, 2014.
- [32] Z. Liu, C. Colin, A. Trentesaux, G. Siani, N. Frank, D. Blamart and S. Farid, "Late Quaternary Climatic Control on Erosion and Weathering in the Eastern Tibetan Plateau and the Mekong Basin," *Quaternary Research*, vol. 63, no. 3, pp. 316-328, 2005.

- [33] R. Schliemann and S. V. Churakov, "Atomic Scale Mechanism of Clay Minerals Dissolution Revealed by Ab Initio Simulations," *Geochimica et Cosmochimica Acta*, vol. 293, pp. 438-460, 2021.
- [34] I. Sevastjanova, R. Hall and D. Alderton, "A Detrital Heavy Mineral Viewpoint on Sediment Provenance and Tropical Weathering in SE Asia," *Sedimentary Geology* , vol. 280, pp. 179-194, 2012.
- [35] B. Jin, M. Wang, W. Yue, L. Zhang and Y. Wang, "Heavy Mineral Variability in the Yellow River Sediments as Determined by the Multiple-Window Strategy," *Minerals*, vol. 9, pp. 85, 2019.
- [36] K. T. Ratcliffe, A. C. Morton, D. H. Ritcey and C. A. Evenchick, "Whole-Rock Geochemistry and Heavy Mineral Analysis as Petroleum Exploration Tools in the Bowser and Sustut Basins, British Columbia, Canada," *Bulletin of Canadian Petroleum Geology*, vol. 55, no. 4, pp. 320-336, 2007.
- [37] S. Andò, S. Aharonovich, A. Hahn, S. C. George and P. D. Clift, "Integrating Heavy- Mineral, Geochemical and Biomarker Analyses of Plio-Pleistocene Sandy and Silty Turbidites: A Novel Approach for Provenance Studies (Indus Fan, IODP Expedition 355)," *Geological Magazine*, vol. 157, no. 6, pp. 929-938, 2019.
- [38] X. Peng, C. Feng and L. Guo, "Sedimentary Geochemistry of the Weihe River Sediments, Central China: Implications for Provenance and Weathering," *Arabian Journal of Geosciences* , vol. 14, pp. 604, 2021.